Rig Design for Meniscus Confinement Method In Metal Additive Manufacturing

[1]Shine George, [2]Sundaresan V L

[1]Lecturer in Automobile Engineering,[2]Lecturer in Mechanical Engineering
[1]Technical Education Department, Kerala
[1]Government Polytechnic College
Kalamassery, India.

***Abstract*- Additive manufacturing or 3D printing is the process of creating 3D objects from digital models through the layer-by-layer deposition of materials. Electrochemical additive manufacturing is a novel non-thermal process capable of producing micro and nano scale metal parts by additive manufacturing. For the additive manufacturing) of metal objects, the powder-based fusion method is routinely utilized to fabricate macro scale parts. The PBF method is limited by fabrication precision due to residual stresses. On the other hand, electrochemical additive manufacturing (ECAM), in which metallic structures are deposited through the electrochemical reduction of metal ions, is a promising technique for producing micro and nano scale objects. This is a relatively new technique which can create metallic components by depositing adherent layers of metal ions onto the surface of conductive substrate. In this meniscus-guided electro deposition approach, a meniscus is formed between the print head and substrate, and electro deposition is confined within the meniscus. This is achieved through the increase of the meniscus diameter to 400 µm which was achieved through the integration of a porous sponge into the print head to balance the hydraulic head of the electrolyte. ECAM uses the principles of electrochemical deposition combined with the additive manufacturing technique to produce parts directly from three-dimensional computer models of the parts. A 3D object is fabricated by the meniscus moving with the print head according to the programmed pattern and the material subsequently being deposited at the designated locations. In this report the design considerations of rig for ECAM based on meniscus confined approach is presented. Different process parameters like applied potential, electrolyte concentration, nozzle diameter etc are coming under study.**

***Index Terms*- Electro chemical additive manufacturing, Metal 3D printing, Printer design.**

I. INTRODUCTION

Additive manufacturing or 3D printing is the process of creating 3D objects from CADD models through layer-by-layer deposition of material on to a substrate. Electro chemical Additive manufacturing (ECAM) is a relatively new form of additive manufacturing method of 3Dmetal printing.In this method, metal deposition is possible by reduction of metal ions from the electrolyte which are deposited onto the surface of a conductive substrate in the form of thin and adherent layers one upon the other in a sequential manner. Electrochemical 3D printing creates metallic structures through electrochemical reduction of metal ions from solution on to conductive substrate. Under ambient condition and without thermal damage, a large range of micro/nano structures can be created. One of the important things is the process is having lower cost as this does not require laser or inert gas set ups which are of high cost. This is the main advantage of this method.

The two approaches of ECAM method are electrochemical deposition 3D printing (LCD) and meniscus confinement method. In localized electrochemical deposition 3D printing (LCD), a sharp tipped electrode act as print head is placed very close to a conductive substrate. The print head, substrate is dipped in the electrolyte. The electrode which is submerged in electrolyte in the print head is connected to positive terminal which acts fully as anode and conductive substrate is connected to -ve terminal act as cathode. In Meniscus Guided Electro Deposition (MGED) or Meniscus confined electro deposition (MCED), a micropipette or a syringe carrying the electrolyte and an electrode is used as print head. When micropipette approaches the conductive substrate, a liquid meniscus is established between these two. The electro deposition is then confined to a small region of the meniscus when appropriate potential difference is applied.

II. OVERVIEW

Electro chemical additive manufacturing (ECAM) by meniscus confined electro deposition (MCED) is a manufacturing process that enables depositing metals from an electrolyte. The metallic structure is created by the formation of a stable liquid meniscus between dispensing nozzle and conductive substrate [1].The print head assembly is a micro pipette or a syringe with micro tip nozzle containing the electrolyte and electrode which act as anode. The conductive substrate act as cathode. When a positive potential is applied between anode and cathode, metal ions flow from anode to cathode, i.e., metal ions are deposited on substrate [8]. The pipette/syringe, nozzle, electrode dipped in electrolyte forms the print head and the electrolyte are dispensed through nozzle [9]. Localized electro deposition is governed by the meniscus –liquid bridge or capillary between pipette tip and the substrate.

The figure 1.1 shows a schematic diagram of an electrochemical 3D printer. The print head is a polyurethane syringe and nozzle of diameter 400µm which is filled with a solution of copper sulphate. A porous sponge is inserted to the nozzle which is inert to the electrolyte. Porous sponge provides sufficient back pressure to the hydraulic head so that a stable meniscus can be formed. Without this sponge, the electrolyte readily flows through the large nozzle and maintaining a stable meniscus becomes difficult.

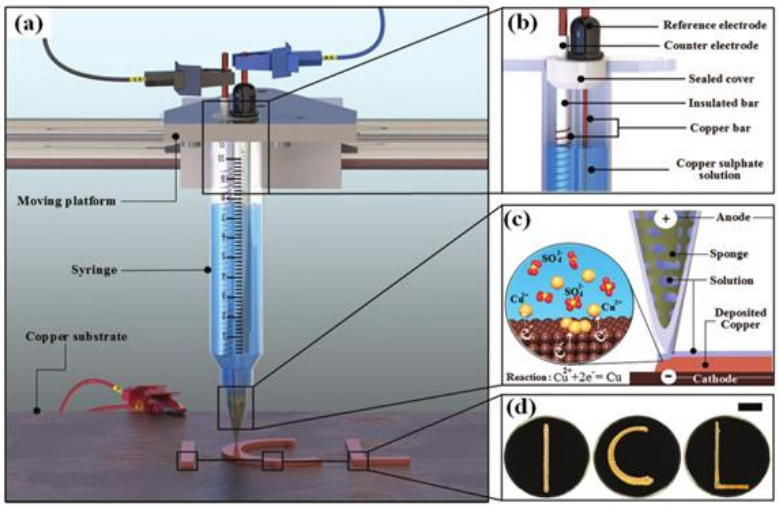

Figure 1.1Schematic illustration of electrochemical 3D printer.

a) Overview of the print head set-up. b) Detailed view of electrode arrangements.

c) Detailed view of the print nozzle highlighting the copper deposition process and the sponge in the tip and d) Optical images of printed copper letters with a potential of 4V Vs Cu

[Picture Source: A Low-Cost Desktop Electrochemical Metal 3D Printer Xiaolong Chen, Xinhua Liu, Peter Childs, Nigel Brandon, and Billy Wu Adv. Mater. Technol. 2017, 2, 1700148 © 2017 WILEY-VCH Verlag GmbH & Co. KGaA, Weinheim]

III. Electrolyte and Applied Potentials

The Electrolyte used is 1mole Cuso4.5H2O and the deposition potentials of 1V to 6V were applied. The time duration of deposition was kept 3600s.After application of various deposition potentials a good and dense structure with high degree of concentricity with ideal morphology is obtained when 1V is applied. A faster deposition rate of copper is obtained while applying 2V. Structure obtained was also good but shape obtained has convexity towards edges from centre. Dendrite formation is apparent when 3V is applied and increased porosity of deposited metal. When 4V is applied, a dendrite structure with finer morphology is obtained at the base as compared to upper regions. The print velocity was 0.4mm/s for all ranges of applied potential and it is found that the thickness of deposited metal line increased from 0.3mm to1.5mm between 1V to 4v for period of 3600s. Beyond this voltage range deposition efficiency found to be decreasing. The Z resolution in this method is high and hence this technique can be used in the fabrication of sensors in electronic circuits. Printed structure exhibits highly poly crystalline structure. Also, in Vickers hardness tests also high range of values 211 to 228 Mpa were obtained and the electrical conductivity ranges from 1.31x106 to 6.86 x 106 S/m [13]

When selecting print head mechanism, the gear assisted rack and pinion mechanism found to be unfeasible as it is difficult to establish a stable meniscus with this where accurate control is necessary[12]. To create a stable meniscus the print head is required to be in contact with the bed or platform and slightly retracted after first contact. Also sponge selection is also critical for balancing hydraulic head. The concentration of electrolyte and applied potential which are the deposition parameters highly influence the morphology of deposited objects. Uneven surfaces are obtained as a result of increased deposition speed and deposition current while increasing deposition potentials. Above 4V the current becomes unstable may be due to detachment of gas bubbles on electrode surfaces [12].

The extrusion system used is gravity based and the electrolyte is extruded through nozzle. The important and key challenge is to maintain and balance static hydraulic head with the pressure drop and surface tension effects [14].

The quantitative evaluation of the sponge length can be calculated by considering the static pressure head.

i.e., $pb - pa = -(Zb - Za)$ eq.(1)

By Darcy's law

$Q = -(KA/\mu)\,[(pb - pa)/L]$ [14] eq.(2

IV. Substrate

The substrates used were unpolished brass plate (67% copper and33% Zinc) having surface roughness Ra=0.017µm, unpolished copper plate having surface roughness 0.19 µm and poly ethylene terephthalate (PET). No reference electrode is used- two electrode systems are used. The deposition voltage was adjusted to 25 V so that current is approximately 0.3mA. Both constant and pulsed potentials were applied for depositing Copper and for Nickel constant potential is used. Relatively larger potential value is used than that used in[12]. The electrolyte needs to pass through a lengthy narrow main channel to the print head tip. Due to the high width to length ratio of main channel, the movement of metal ions from reservoir to the tip of the print head is limited[16]. The resistance of whole circuit is found to be increased as the concentration of metal ions through main channel is lower than that in reservoir.

V. METHODOLOGY

Meniscus confined electro deposition (MCED) is an additive manufacturing process that enables depositing metals from an electrolyte containing nozzle (pipette) in an arbitrary 3D pattern. Here the hot end print head of a FDM 3D printer is replaced with a 3D printer with the hot end is replaced with a 20ml polypropylene dispensing syringe with a 400µm polypropylene nozzle which is held on the same carriage where printer hot end was fixed. The syringe is filled with electrolyte (CuSo4). Copper rod is dipped in to it and is connected to positive terminal of power supply. A copper plate of dimensions 100 x 25 mm is fixed on print bed is used as substrate which is connected to negative terminal of power supply.

Copper sulphate electrolytes are prepared by mixing 1 mole Cu So4.5H2O with deionised water for copper deposition. Here for first trial, 25 g Cu So4.5H2O is mixed with deionised water. In subsequent investigation 1.5 mole concentrations were done.

VI. RIG DESIGN

Here new extrusion system which is simply gravity-based is introduced. The electrolyte is extruded through nozzle which is governed by the formation of a stable meniscus and entrainment from the lateral movement of the print head. To maintain and balance the
static hydraulic head with the pressure drop through the nozzle and the surface tension effects is a challenge. A porous sponge is used to adjust the pressure drop in the nozzle to the appropriate amount.

The quantitative evaluation of the sponge length can be calculated by considering the static pressure head as referred in equation (1) and flow rate from equation (2)

VII. FORMATION OF STABLE MENISCUS

For maintaining and balancing the head and stable meniscus, sponge cubes with dimensions of 10 x 10 x 10 mm were compressed into the nozzle head. Porous is sponge used in this study is made of polyurethane. The porosity (ϕ) of the uncompressed sponge was measured to be 0.59 (where 1 is complete void and 0 is completely dense). To form a stable and well controlled meniscus, a sponge filled nozzle is first created. In this work, for a 400 µm diameter nozzle with a 1 M copper sulphate solution, 1 cm3 of polyurethane sponge with an uncompressed porosity of 0.59 was used.

VIII. EXPERIMENTAL SET UP

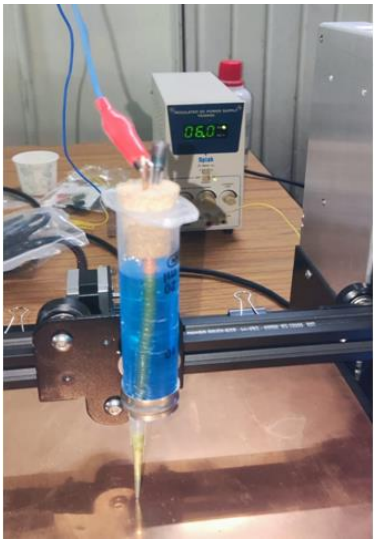

Figure 3.1 Experimental set-up Modified printer with hot end print head replaced with polyurethane syringe filled with electrolyte.

In the singe dots experiments, a 1 M CuSO4 electrolyte was prepared by combining 12.5 g ofCuSO4 · 5H2O (Sigma Aldrich) and 50 ml of deionised water. The copper substrate was
prepared by cutting a 100 x 25 x 0.3 mm pure copper sheet. The substrate was cleaned with acetone and deionised water before use. Deposition duration was fixed at 3600s for all experiments. Temperature and humidity were at room conditions which were 20 °C and30%-45% respectively. The nozzle was placed firmly to substrate without electrolyte leaking. For single lines, the deposition conditions and electrolyte were prepared similarly as single dots. The nozzle was controlled to move along X axis by a distance of 10 mm and 3600 s duration with a speed of 400µm/s.
The nozzle/syringe assembly(print head) is mounted on a carriage of the 3D printer by replacing the hot end (figure3.1,3.2) .Copper rod is dipped in the copper sulphate electrolyte and act as a counter electrode. The counter electrode is held in an insulated holder to maintain dimensional accuracy with the end of the copper rod attached to the copper wire which is wrapped around insulated holder. For creating an initial structure, the print head is moved towards the print bed and made to contact with the copper substrate and retracted to a small distance so that a stable meniscus is developed in between them. The working electrode which is connected to copper plate and counter electrode submerged in electrolyte. A positive potential is then applied between them and due to the

applied potential copper ions are separated. i.e., reduction of Cu2+ ions from electrolyte (CuSO4) happens and are deposited onto the substrate through the nozzle. At the same time the Cu2+ ions are replenished from the counter electrode to the electrolyte by the oxidation reaction to form a concentration gradient between counter and working electrode controlled through a combination of diffusion and migration

The print head/ Nozzle assembly is then moved in the X- and y-directions in a defined tool path generated based on the 3D computer model. The letter A of size 20x20x1mm made from CADD software and the file is converted to STL format, sliced using CURA software. The thickness designed is 1mm,no. of layers is 10, each layer thickness 0.1 mm height. The print speed is set at 400 µm/s. Fabrication of letter A was performed using a copper sulphate concentration of 1 M with deposition voltage 4 V versus Cu under ambient conditions

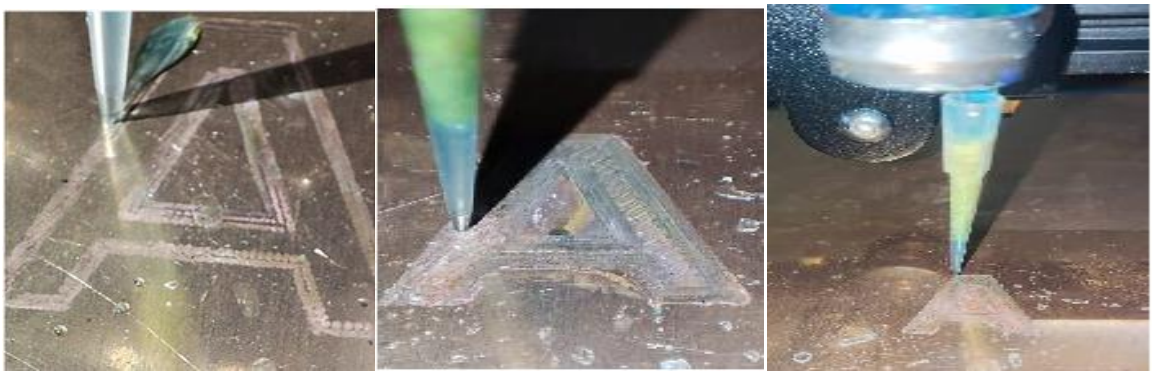

(a) (b) (c)

Figure 3.3 (a), (b), (c) Printing of letter A

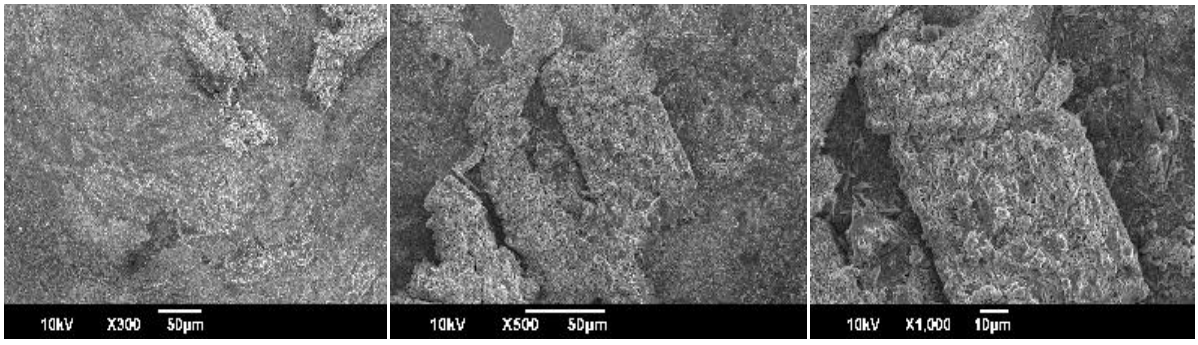

(a) (b) (c)

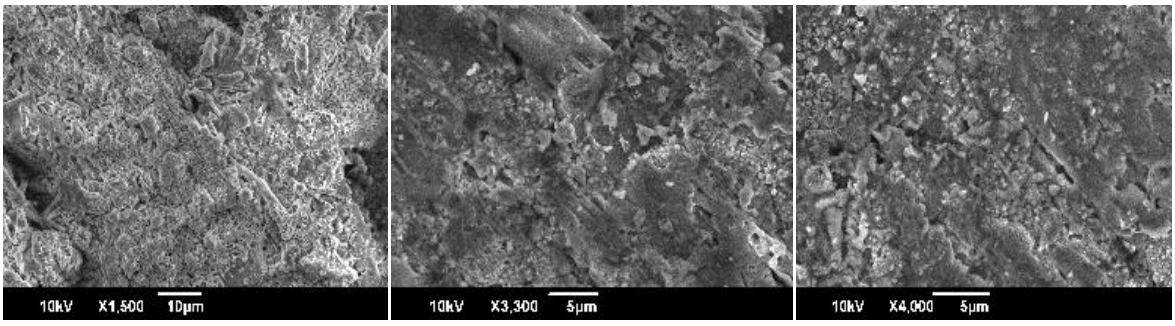

(d) (e) (f)

Figure 3.4 The SEM images of Printed letter A

It is obvious from the SEM images that the deposition morphology is not in a dendritic manner which suggests that the relative position of the print head aids with mass transport of copper ions or mechanical removal of the dendrites. For a 1 h deposition it is be observed that the thickness of printed structure letter A, the deposition efficiency is low and hence there is a decrease in deposited material while the lateral speed is at 0.4 mm/s, the line thicknesses is 1mm.

Printing of dots and wires (pillars) were performed using 1 molar and 1.5 molar concentrated copper sulphate solution with deposition voltages ranging from 1 to 6 V and nozzle diameters 0.4 mm and 1mm under ambient conditions. Figure 3.5 shows the printing of dots at 2V deposition voltage and 1 mol electrolyte concentration. Here deposition rate is too slow. 0.2 to 0.25 mm height is obtained after 1 hr deposition.

(a) (b)

Figure 3.5 Printed dots at 2V deposition voltage and 1 molar electrolyte concentration

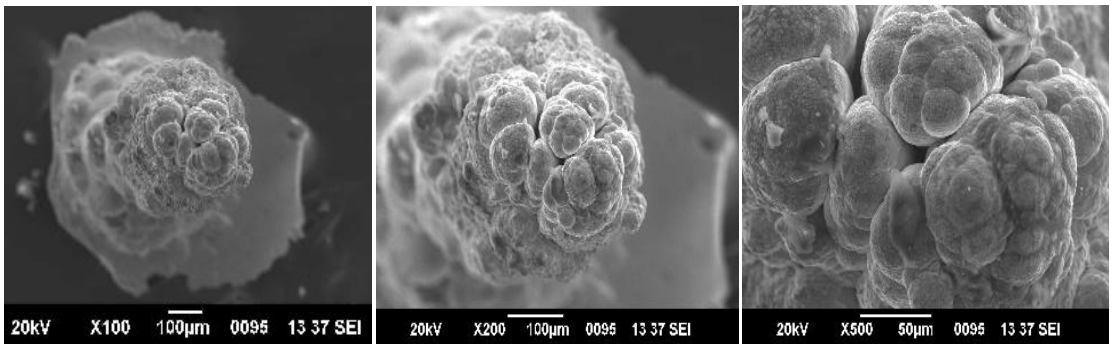

(a) (b) (c)

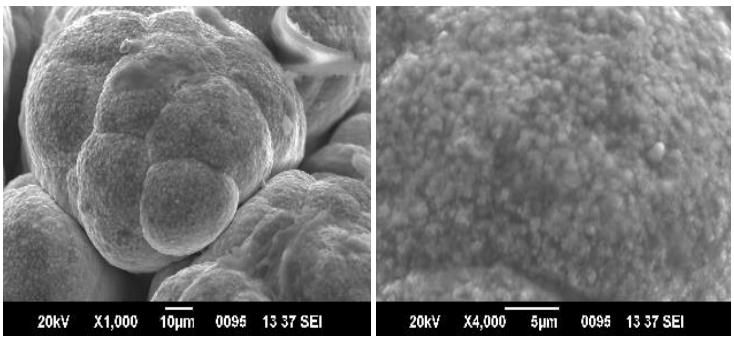

(d) (e)

Figure 3.6 The SEM images of dots printed at 2V deposition voltage and 1molar electrolyte concentration.

Printing of dots and wires (pillars) were conducted with 1 molar concentrated copper sulphate solution and deposition voltages ranging from 2,3,4,5 and 6 V under ambient conditions. Figure 3.6 (a to e) shows the SEM images of the printed dots with a deposition time of 1 h. Of the samples, the 2 V deposition shows a cauliflower like dense structure and high degree of concentricity due to the meniscus confinement approach. A faster rate of growth with a dense structure was observed in this sample according to SEM images. A convex shape at the centre is observed and may be due to preferential deposition there.

(a) (b)

Figure 3.7 Figure 3.7 shows the printing of dots at 3V deposition voltage and 1 mol electrolyte concentration. Here also deposition rate is slower one. Deposition height of 2 to 2.5 mm is achieved after 1 hr.

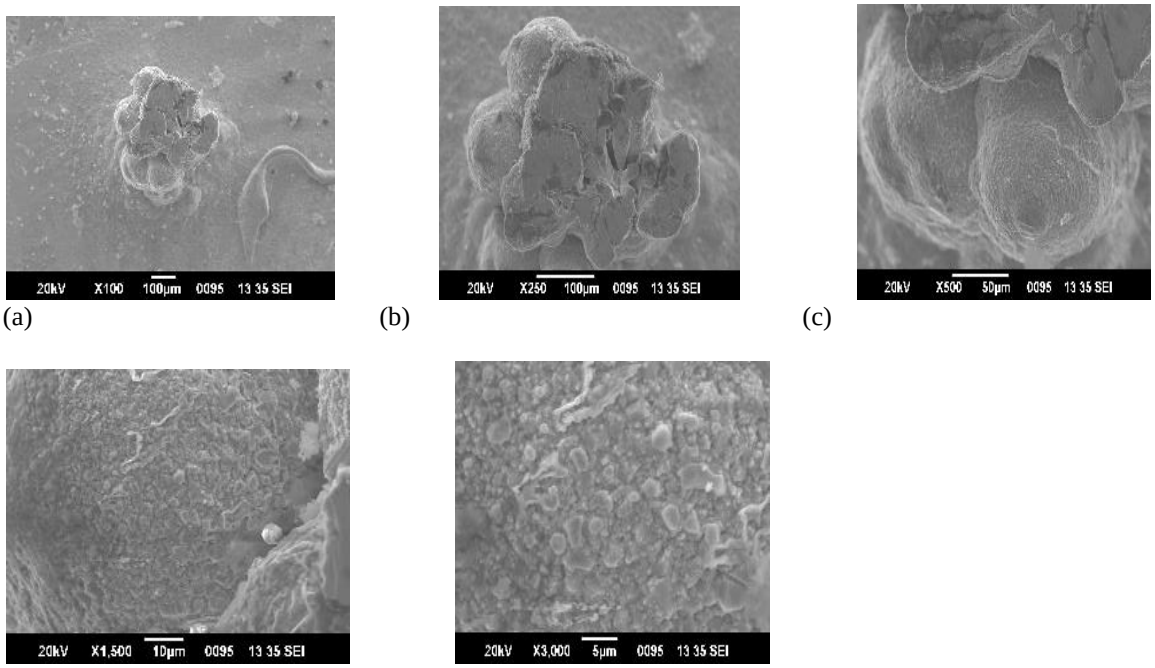

(a) (b) (c)

(d) (e)

Figure 3.8

Figure 3.8 (a to e) shows the SEM images of dots printed at 3V deposition voltage and 1 mol electrolyte concentration. The formation of copper dendrites observed clearly visible due in the printed dot. Here the structure obtained is somewhat dense as obtained with 2V applied potential with same concentration of electrolyte.

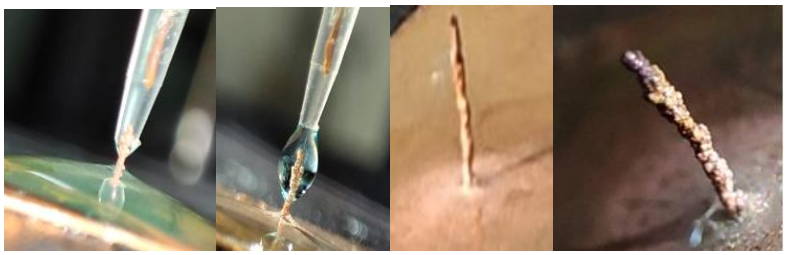

(a) (b) (c) (d)

Figure 3.9

Figure 3.9 shows the printing of wire at 4V deposition voltage and 1 molar electrolyte concentration. In this case deposition rate is more than previous ones. 5 to 6 mm height wires are fabricated during 1 hr deposition.

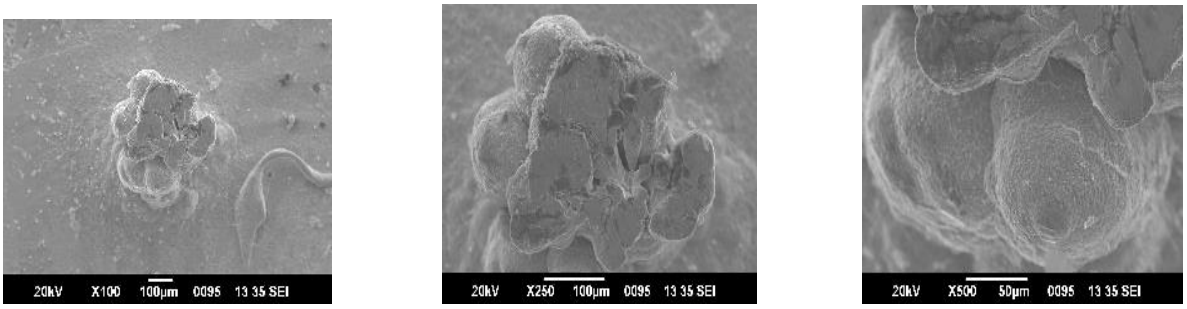

(a) (b) (c)

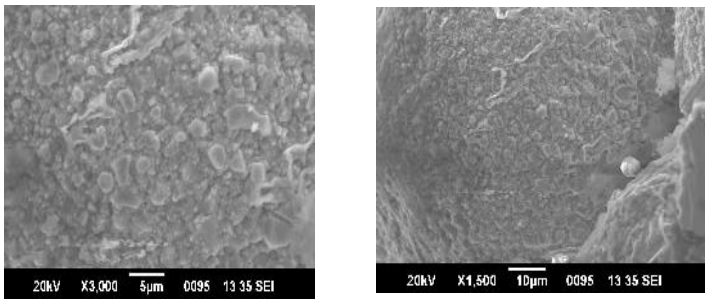

(d) (e)

Figure 3.10

Figure 3.10 (a to e) shows the SEM images of dots printed at 4V deposition voltage for 1 molar concentration of electrolyte. At 4 V applied potential. The SEM images shows that porosity continuing to increase with increasing deposition potential.

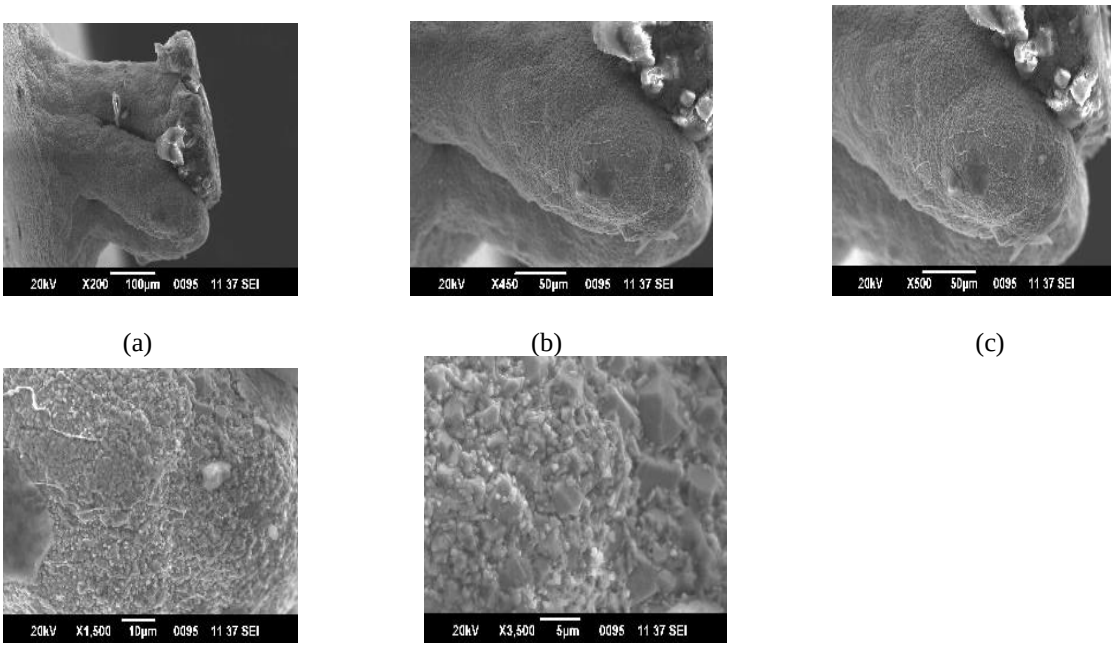

(a) (b) (c)

(d) (e)

Figure 3.11

The SEM images of wires printed at 4V deposition voltage and 1 mol electrolyte concentration

Figure 3.12
Figure 3.12 shows the printing of wire at 5V deposition voltage and 1 mol electrolyte concentration. In this case deposition rate is more than previous ones. 5 to 6 mm height wires are fabricated during 1 hr deposition. But the structure obtained is more porous than previous ones

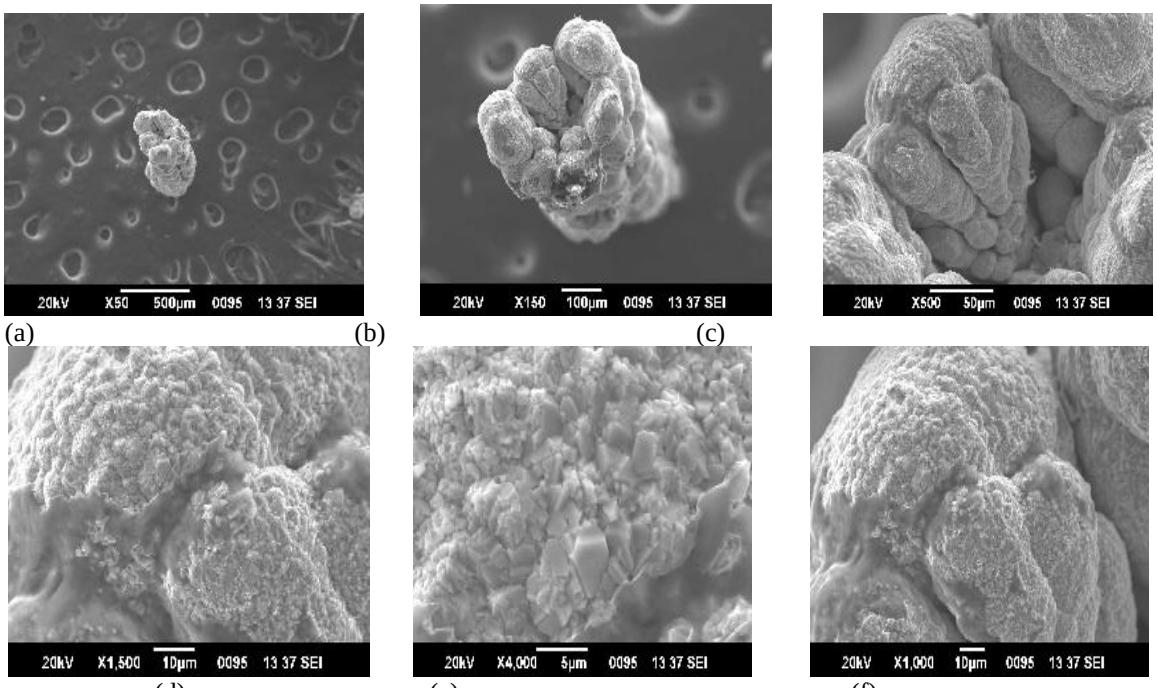

(a) (b) (c)

(d) (e) (f)

Figure 3.13

The SEM images of wires printed at 5V deposition voltage and 1 mol electrolyte concentration

At 5 V applied potential porosity is found to be more than other applied lower potentials according to the SEM images . The deposition becomes more porous at higher regions. This suggests that the porosity of printed structure continuing to increasing with increasing deposition potential.

Figure 3.14
The printed of dot at 2V deposition voltage and 1.5 molar electrolyte concentration,
1 mm nozzle diameter

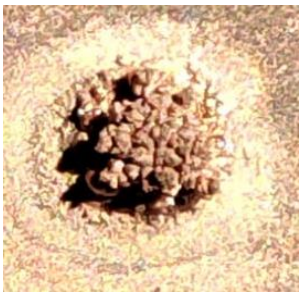

Figure 3.15
The printed of dot at 3V deposition voltage and 1.5 molar electrolyte concentration,
1 mm nozzle diameter

Figure3.16
The printed of dot at 4V deposition voltage and 1.5 molar electrolyte concentration,
1 mm nozzle diameter

Figure3.17
The printed of dot at 5V deposition voltage and 1.5 molar electrolyte concentration,
1 mm nozzle diameter

Figure 3.18
The printed of dot at 6V deposition voltage and 1.5 molar electrolyte concentration,
1 mm nozzle diameter

IX. MICRO HARDNESS TEST

Mitutoyo HM 200 Series micro-Vickers hardness machine is used for testing the micro hardness of specimen .A minimum load of 10 gmf (100 mN) and maximum of 2 kgmf (20,000 mN) was applied to test the hardness of the single dots. Silicon carbide paper with grade of 1500 was used to polish all samples. Then, samples were prepared and mounted into an epoxy resin for the indentation test. During the experiments, a load of 10, 250, 500, 750, 1000 gmf were applied to all samples with creep time of 10seconds. For the Vickers-indentation test, the tip angle was 136°. The diagonal length of the contact area can be used to calculate the HV value using the below formula:

Vickers Number ,HV = 2F (Sin (1360/2))/ $d2$

$$= (0.1891F/d2)$$

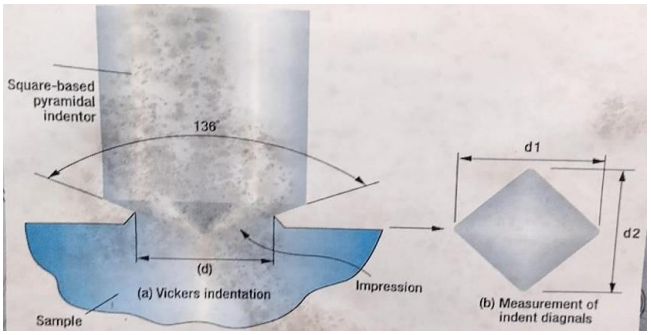

Figure 3.19

X. Results and Discussions

It is obvious from the SEM images that the deposition morphology is not in a dendritic manner in the case of printed letter A . For a 1 h deposition it is be observed that the thickness of printed structure, the deposition efficiency is low for letter A and hence there is a decrease in deposited material while the lateral speed is at 0.4 mm/s, the line thicknesses is 1mm. Printing of dots and wires (pillars) were performed using 1 molar and 1.5 molar concentrated copper sulphate solution with deposition voltages ranging from 1 to 6 V and nozzle diameters 0.4 mm and 1mm under ambient conditions. Figure 3.5 shows the printing of dots at 2V deposition voltage and 1 mol electrolyte concentration. Here deposition rate is too slow. 0.2 to 0.25 mm height is obtained after 1 hr deposition.

Printing of dots and wires (pillars) were conducted with 1 molar concentrated copper sulphate solution and deposition voltages ranging from 2,3,4,5 and 6 V under ambient conditions. Figure 3.6 (a to e) shows the SEM images of the printed dots with a deposition time of 1 h. Of the samples, the 2 V deposition shows a cauliflower like dense structure and high degree of concentricity due to the meniscus confinement approach. A faster rate of growth with a dense structure was observed in this sample according to SEM images. A convex shape at the centre is observed and may be due to preferential deposition there.

Figure 3.7 shows the printing of dots at 3V deposition voltage and 1 mol electrolyte concentration. Here also deposition rate is lower one. Deposition height of 2 to 2.5 mm is achieved after 1 hr. Figure 3.8 (a to e)shows the SEM images of dots printed at 3V deposition voltage and 1 molar concentration of electrolyte. The formation of copper dendrites observed clearly visible due in the printed dot. Here the structure obtained is somewhat dense as obtained with 2V applied potential with same concentration of electrolyte.

Figure 3.9 shows the printing of wire at 4V deposition voltage and 1 molar electrolyte concentration. In this case deposition rate is more than previous ones. 5 to 6 mm height wires are fabricated during 1 hr deposition. Figure 3.10 (a to e) shows the SEM images of dots printed at 4V deposition voltage for 1 molar concentration of electrolyte. At 4 V applied potential. The SEM images shows that porosity continuing to increase with increasing deposition potential

Figure 3.11(a to e) shows the SEM images of wires printed at 4V deposition voltage and 1 mol electrolyte concentration. Figure 3.12 shows the printing of wire at 5V deposition voltage and 1 mol electrolyte concentration. In this case deposition rate is more than previous ones. 5 to 6 mm height wires are fabricated during 1 hr deposition. But the structure obtained is more porous than previous ones

Figure 3.13 (a to f) shows the SEM images of wires printed at 5V deposition voltage and 1 mol electrolyte concentration. At 5 V applied potential porosity is found to be more than other applied lower potentials according to the SEM images. The deposition becomes more porous at higher regions. This suggests that the porosity of printed structure continuing to increasing with increasing deposition potential.

Also, Vickers hardness tests of printed specimen reveals that hardness decreases with higher applied potentials but increases with higher concentration of electrolyte. From the Hardness values of printed wires / pillars it can be observed that the hardness of printed copper ranges from 50 to 176 HV for 1 molar concentration of electrolyte and 59 to 198 HV for 1.5 molar concentration of electrolyte.

Table 4.1

Hardness values of specimen at 1 M concentration and plain plate					
Applied load gmf	3 V	4 V	5 V	6 V	Plain Plate
10	127.2	148	77.2	86.5	115.3
250	181.5	136.3	98.4	93.3	90.7
500	155.8	144.7	76.4	61.5	80.7
750	122.8	95	77.4	49.2	73
1000	110	129.3	64.4	70.6	59.7

Table 4.1 shows the results of micro hardness test conducted of specimen for 1M concentration of electrolyte and hardness values of plain copper plate.

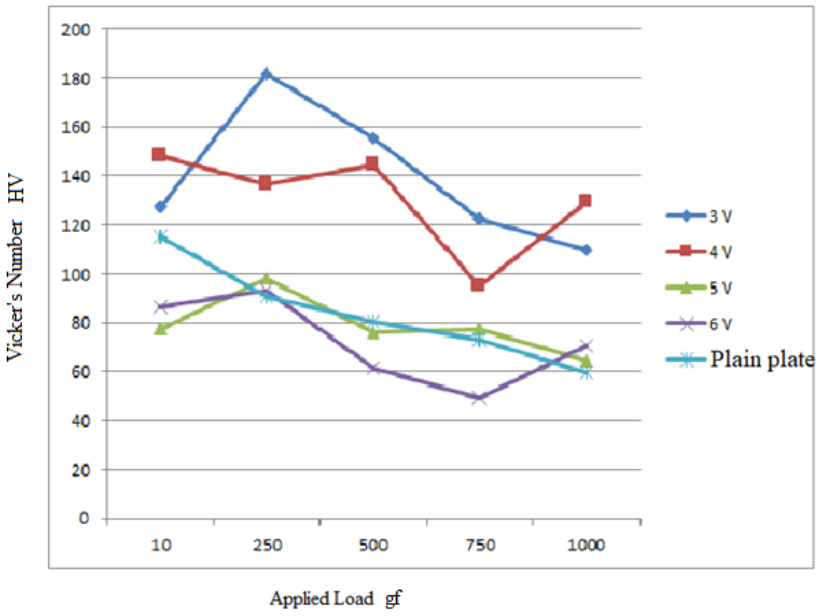

Figure 4.1 shows the graph with Applied load (gf) Vs Vickers Number (HV) at different potentials applied for 1M concentration of electrolyte

Table 4.2

Hardness values of specimen at 1.5 M concentration and plain plate					
Applied load gf	3 V	4 V	5 V	6 V	Plain Plate
10	107.7	95.7	107.6	138.8	115.3
250	163.6	72.5	127.1	167.2	90.7
500	148.5	103.2	115.6	198.5	80.7
750	144.1	81.3	142.5	143.3	73
1000	107.4	107.3	115.6	169.2	59.7

Table 4.2 shows the results of micro hardness test conducted of specimen for 1.5M concentration of electrolyte

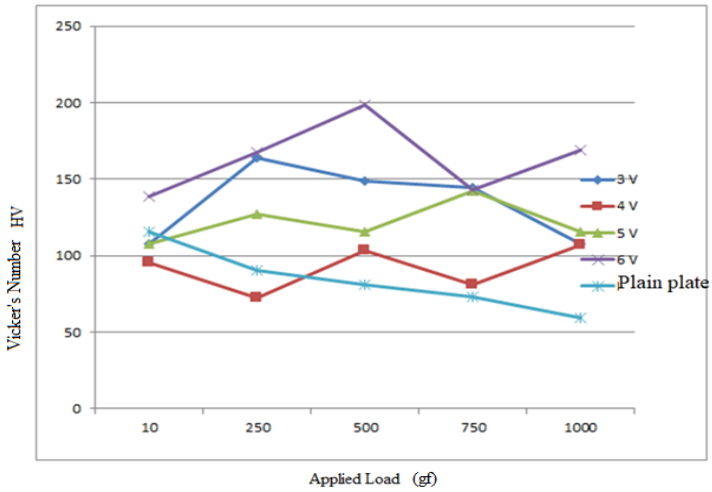

Figure 4.2 shows the graph with Applied load (gf) Vs Vickers Number (HV) at different potentials applied for 1.5M concentration of electrolyte

Table 4.3

Hardness Values (HV)		
Applied Potential (V)	concentration of electrolyte	
	1 m	1.5 m

3	155.8	148.5
4	144.7	103.2
5	76.4	115.6
6	61.5	198.5

Table 4.3 shows the Vickers Number (HV) of specimen for 1m &1.5 m concentration of electrolyte at an applied load of 500gf

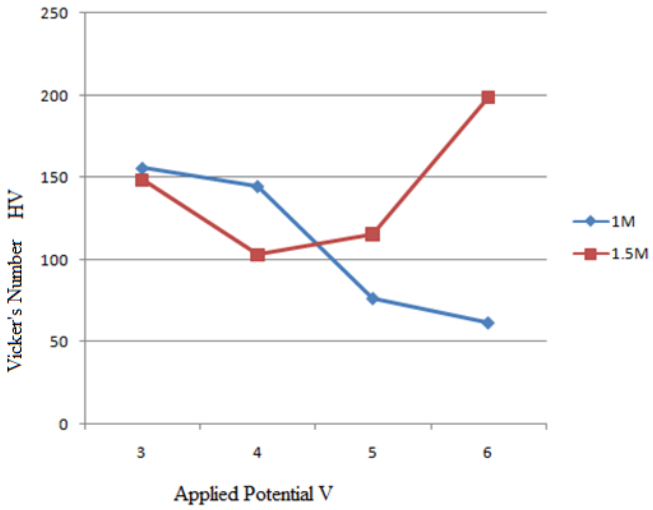

Figure 4.3

Figure 4.3 shows the graph with Applied Potential (V) Vs Vickers Number (HV) at different for concentration of electrolyte (1M, 1.5M) at an applied load of 500gf.

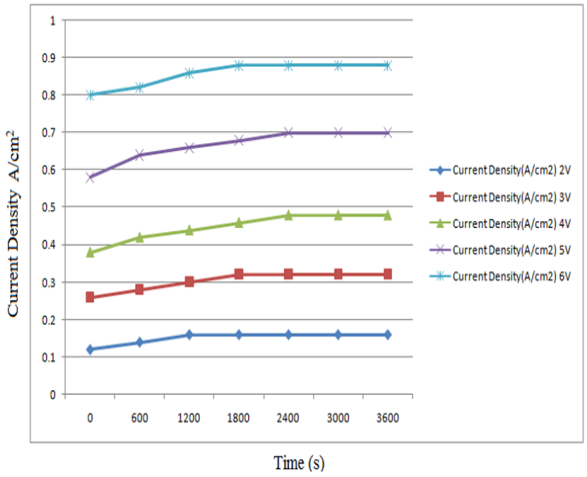

Figure 4.4

Figure 4.4 shows the graphical representation of Time (s) Vs Current Density (A/cm2) of single dot and wires, 1 M electrolyte concentration

XI. CONCLUSIONS

The rig design for ECAM based on meniscus confined method for metal 3D printer is presented. This work presents a design for low-cost ECAM system for printing micro/nano scale metal parts. The print head which is significantly larger here than other designs. The use of a porous sponge helps to create a sufficient back pressure for the hydraulic head created by the electrolyte in the micropipette/syringe. Higher volumetric deposition rates achieved compared with other ECAM approaches especially in the case of printing of wires/ pillars. The influence of deposition potential and concentration important for copper deposition from an aqueous copper sulphate solution. Here the copper is attempted to print from copper sulphate solution. Nickel, silver and Titanium, can be printed through the same ECAM system from their aqueous solution as electrolyte.

The surface smoothness can be controlled by manipulating the applied potential and printing strategy. The presented work explains the possibility to control the meniscus and electrolyte flow by designing an appropriate micro fluidic system to achieve higher printing precisions and satisfactory material properties for the fabrication of functional electronics. It is observed that evaporation has a significant effect in the process. By lowering the relative humidity (RH) of the environment, it is noted that flux of ions toward the cathode increased which was due to the increased evaporation rate from the meniscus surface. In addition, the

evaporation process generated a convective flow in the nozzle that influenced the concentration of the ions at the cathode surface, which controls the growth rate of the microwire. Determining and establishing the highest growth rate for fabrication of uniform metallic structures can be challenging in experiment since it depends on various factors, e.g., type of electrolyte, concentration of the electrolyte, size of pipette, desire radius and height of the wire, and temperature and pressure of the system.

From Time Vs current density graph (figure 4.4) it is observed that current density has lower values during the first 1200s of 3600s of total deposit time. This may be due to variation in current due to resistance of electrolyte. It is also observed during all investigation that deposition rate is too low for all applied potentials and electrolyte concentration during first 1200s of deposition time. This may also be due to the variation of current due to resistance of electrolyte. From this investigation it is observed that when diameter of nozzle increases, the deposition rate decreases and the nozzle speed influences shape of liquid meniscus between the tip of the nozzle and the growth front and beyond a certain range, meniscus becomes unstable, which stops the deposition process also the porosity of deposited part increases. The deposition is found to be poor in the case of letter printing and hence it is recommended that the nozzle speed is to be kept optimum.

REFERENCES:

1. Chen, Xiaolong, et al. "A low cost desktop electrochemical metal 3D printer." Advanced Materials Technologies 2.10 (2017): 1700148.
2. Skowyra, Justyna, Katarzyna Pietrzak, and Mohamed A. Alhnan. "Fabrication of extended-release patient-tailored prednisolone tablets via fused deposition modelling (FDM) 3D printing." European Journal of Pharmaceutical Sciences 68 (2015): 11-17.
3. Manfredi, D., et al. "Direct metal laser sintering: an additive manufacturing technology ready to produce lightweight structural parts for robotic applications." La metallurgia italiana (2013).
4. Ambrosi, Adriano, and Martin Pumera. "3D-printing technologies for electrochemical applications." Chemical society reviews 45.10 (2016): 2740-2755.
5. Murr, Lawrence E., et al. "Fabrication of metal and alloy components by additive manufacturing: examples of 3D materials science." Journal of Materials Research and technology 1.1 (2012): 42-54.
6. Ding, Donghong, et al. "Wire-feed additive manufacturing of metal components: technologies, developments and future interests." The International Journal of Advanced Manufacturing Technology 81 (2015): 465-481.
7. Ding, J., et al. "Thermo-mechanical analysis of Wire and Arc Additive Layer Manufacturing process on large multi-layer parts." Computational Materials Science 50.12 (2011): 3315-3322.
8. Madden, John D., and Ian W. Hunter. "Three-dimensional microfabrication by localized electrochemical deposition." Journal of microelectromechanical systems 5.1 (1996): 24-32.
9. Hu, Jie, and Min-Feng Yu. "Meniscus-confined three-dimensional electrodeposition for direct writing of wire bonds." Science 329.5989 (2010): 313-316.
10. Morsali, Seyedreza, et al. "Multi-physics simulation of metal printing at micro/nanoscale using meniscus-confined electrodeposition: Effect of environmental humidity." Journal of Applied Physics 121.2 (2017).
11. Seol, Seung Kwon, et al. "Electrodeposition-based 3D printing of metallic microarchitectures with controlled internal structures." Small 11.32 (2015): 3896-3902.
12. Chen, Xiaolong, et al. "A low cost desktop electrochemical metal 3D printer." Advanced Materials Technologies 2.10 (2017): 1700148.
13. Chen, Xiaolong, et al. "A low cost desktop electrochemical metal 3D printer." Advanced Materials Technologies 2.10 (2017): 1700148.
14. Chen, Xiaolong, et al. "A low cost desktop electrochemical metal 3D printer." Advanced Materials Technologies 2.10 (2017): 1700148.
15. Liu, Pengpeng, et al. "A low-cost electrochemical metal 3d printer based on a microfluidic system for printing mesoscale objects." Crystals 10.4 (2020): 257.
16. Hoshyargar, Vahid, Seyed Nezameddin Ashrafizadeh, and Arman Sadeghi. "Diffusioosmotic flow in rectangular microchannels." Electrophoresis 37.5-6 (2016): 809-817.
17. Chen, Xiaolong, et al. "Multi-metal 4D printing with a desktop electrochemical 3D printer." Scientific reports 9.1 (2019): 3973.
18. Sundaram, Murali M., Abishek B. Kamaraj, and Varun S. Kumar. "Mask-less electrochemical additive manufacturing: a feasibility study." Journal of Manufacturing Science and Engineering 137.2 (2015): 021006.
19. Madden, John D., and Ian W. Hunter. "Three-dimensional microfabrication by localized electrochemical deposition." Journal of microelectromechanical systems 5.1 (1996): 24-32.
20. Said, R. A. "Localized electro-deposition (LED): the march toward process development." Nanotechnology 15.10 (2004): S649.
21. Je, Jung Ho, Jong-Man Kim, and Justyn Jaworski. "Progression in the fountain pen approach: from 2D writing to 3D free-form micro/nanofabrication." Small 13.2 (2017): 1600137.
22. Hu, Jie, and Min-Feng Yu. "Meniscus-confined three-dimensional electrodeposition for direct writing of wire bonds." Science 329.5989 (2010): 313-316.
23. Morsali, Seyedreza, et al. "Multi-physics simulation of metal printing at micro/nanoscale using meniscus-confined electrodeposition: Effect of environmental humidity." Journal of Applied Physics 121.2 (2017).

24. Li, Xinchao, et al. "Review of additive electrochemical micro-manufacturing technology." International Journal of Machine Tools and Manufacture 173 (2022): 103848.